

## Structural control of the surface-frozen layer in alcohol melts

O Gang<sup>†</sup>, B M Ocko<sup>‡</sup>, X Z Wu<sup>§</sup>, E B Sirota<sup>||</sup> and M Deutsch<sup>†¶</sup>

<sup>†</sup> Physics Department, Bar-Ilan University, Ramat-Gan 52900, Israel

<sup>‡</sup> Physics Department, Brookhaven National Laboratory, Upton, NY 11973, USA

<sup>§</sup> IBM Almaden Research Center, San Jose, CA 95120, USA

<sup>||</sup> Exxon Research and Engineering Company, Annandale, NJ 08801, USA

E-mail: deutsch@mail.biu.ac.il

Received 10 September 1999

**Abstract.** Surface crystallization in alcohol melts results in the formation of a crystalline bilayer at the melt's surface *above* the freezing temperature. We demonstrate here that the structure of this surface-frozen bilayer can be varied using specific bulk additives, water and diols. Surface-specific x-ray methods show that water swells the bilayer by intercalating into its centre at a molecular water:alcohol ratio of  $\sim 1:2$ . It also induces surface freezing at chain lengths not showing the effect when dry. Diols are found to induce a reversible monolayer–bilayer surface phase transition. The surface phase diagram is determined and found to depend on the diol's chain length and concentration, in addition to temperature. The physics underlying the phase behaviour is discussed.

### 1. Introduction

Surface molecules are less confined, and hence have higher entropy, than those of the bulk. Thus, surfaces are expected to melt at a lower temperature than the bulk. Such surface melting was indeed found in many solids, including metals, semiconductors, and ice. By contrast, surface freezing (SF), where a crystalline surface phase forms at a temperature  $T_s$  *above* the bulk freezing one,  $T_b$  [1, 2], was discovered only a few years ago in melts of chain molecules [1–3]. In alcohols ( $C_nH_{2n+1}OH$ , denoted as  $C_nOH$ ), a crystalline bilayer forms at the melt's surface at  $T_s \approx T_b + 1$  °C, for  $16 \leq n \leq 28$ . This bilayer is stabilized by hydrogen bonds (HB) between the alcohols' hydroxyl groups, which were found to reside at the bilayer's centre [3].

SF layers differ fundamentally from both water-supported Langmuir monolayers [4] (LM), and self-assembled monolayers (SAM) on solids [5], the two most-studied organic thin films. Unlike LMs, which are confined to the water surface by hydrophobic repulsion, the SF layer's molecules are identical with those of the bulk and can freely exchange with it. Unlike SAMs, the SF layer does not acquire its order by epitaxial attachment to an existing ordered crystalline surface. This new type of thin film is important not only for basic science, but also for the same potential applications (molecular electronics, sensor technology, and nanostructures) as are envisaged for SAMs and LMs.

We have explored the possibility of controlling the SF layer's structure in alcohol melts by varying the HB strength through bulk admixture with small amounts of HB-forming molecules. Two such molecules were studied: first, the obvious choice, water; the second is the  $\alpha$ ,  $\omega$ -diol, (OH– $C_mH_{2m}$ –OH). As it consists of a hydrocarbon chain with one hydroxyl group on each

¶ Author to whom any correspondence should be addressed.

terminal carbon, it allows one to vary the strength ratio of the HB to the chain–chain van der Waals interaction by varying  $m$ . We find that water intercalates into the centre of the SF bilayer, swells it, and lends it an increased stability manifested in larger existence ranges in  $n$  and  $T$ . Diols do not intercalate, probably due to the hydrophobic repulsion between the alcohols' hydroxyls and the diol's alkyl chain. However, they induce a variation in the molecular tilt dependent on the diol concentration ( $\phi$ ), a reversible monolayer–bilayer phase transition, driven by either  $T$ - or  $\phi$ -variation, and an  $m$ -dependent surface phase diagram.

## 2. Experimental procedure

X-ray reflectivity (XR), grazing-incidence diffraction (GID), and Bragg rod (BR) measurements were used to study the free surface's structure in alcohol melts, employing synchrotron radiation at beamline X22B, NSLS. When a surface layer forms, having an electron density,  $\rho_e$ , different from that of the bulk, Kiessig fringes appear in the reflectivity curve,  $R(q_z)$ , where  $q_z$  is the surface-normal momentum transfer. The fringes' period is inversely proportional to the layer's thickness. GID probes the structure within surface plane, and, for a crystalline surface, exhibits sharp diffraction peaks characteristic of the in-plane order. The BR, i.e. the surface-normal intensity distribution at the GID peak position, yields information on the length and the tilt of the molecules.

The >99% pure alcohols were obtained commercially, and used as received. A  $\sim 0.5$  g sample was placed on a flat copper wafer inside a sealed cell, the temperature of which was regulated to  $\leq 0.005$  °C. For hydration, the sample was kept under saturated water vapour throughout the measurement. Diolated samples were prepared by direct mixing of the two components. Further details are given in references [2, 7, 9].

## 3. Results and discussion

### 3.1. Hydrated alcohols

Figure 1(a) shows  $R(q_z)$  for both dry and hydrated  $C_{22}OH$ , normalized to the Fresnel reflectivity,  $R_F$ , of an ideal surface [7]. The shorter Kiessig fringes period of wet  $C_{22}OH$

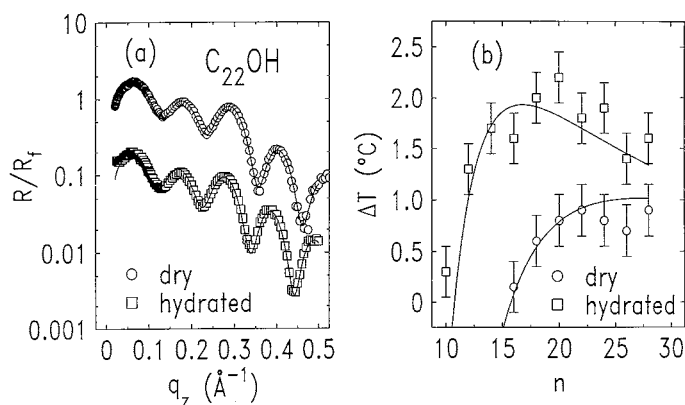


**Figure 1.** (a) Fresnel-normalized x-ray reflectivity for dry and hydrated  $C_{22}OH$ . (b) The variation of the existence range of  $T$  with the molecular length  $n$ . Note the increased range in  $\Delta T$  and  $n$  for the hydrated alcohols.

indicates layer swelling, found to be a uniform  $\sim 2.5 \text{ \AA}$  for all chain lengths  $n$ . Modelling  $R(q_z)$  [3] (solid lines) yields an increase in  $\rho_e$  at the wet bilayer's centre, corresponding to  $\sim 1$  water molecule per pair of upper and lower alcohol molecules in the bilayer. While this 1:2 hydration ratio agrees well with that of the solid bulk [6], it is, surprisingly, *larger* than the  $\sim 1:4$  ratio of the bulk's *liquid* phase [6]. This variation was shown [3] to account quantitatively (solid lines in figure 1(b)) for the almost twofold increase in the temperature range of existence,  $\Delta T = T_s - T_b$ , observed in figure 1, for the wet SF layer, as compared to the dry one, for all  $n$ . The increased SF phase stability, indicated by the larger  $\Delta T$ , results also in a  $\sim 50\%$  larger range of molecular lengths  $n$  showing the SF effect:  $10 \leq n \leq 28$ . For further details on both experiment and theory, see Gang *et al* [3].

### 3.2. Diluted alcohols

The most dramatic effect of the diols is a reversible monolayer–bilayer phase transition in the SF layer, induced by varying either  $T$  or  $\phi$ , as shown in figure 2(a) for a 1, 3-propanediol (PD) (5%):C<sub>22</sub>OH mixture. At  $T \approx 70 \text{ }^\circ\text{C} \gg T_f \approx 66.3 \text{ }^\circ\text{C}$ ,  $R(q_z)$  exhibits the monotonic, smooth fall-off, characteristic of a structureless liquid surface [7, 8]. At  $T \approx 67.5 \text{ }^\circ\text{C}$ , close to but above  $T_f$ , Kiessig fringes typical of a surface bilayer are observed. This curve is practically identical with that of pure C<sub>22</sub>OH, indicating that unlike in hydration, no swelling occurs upon

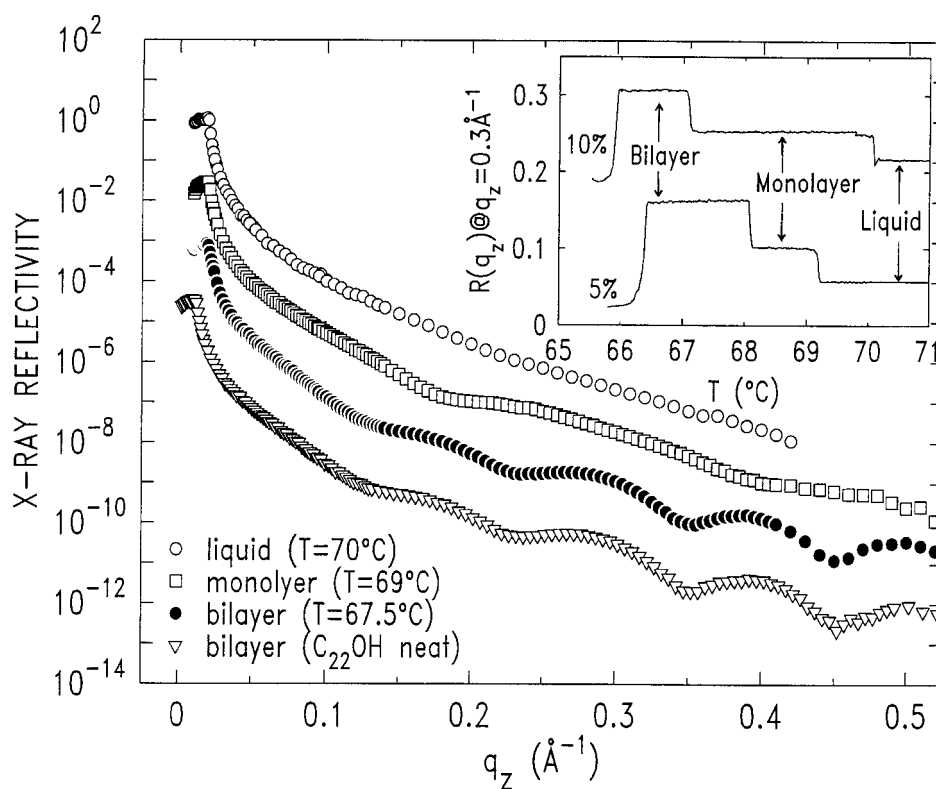


**Figure 2.** X-ray reflectivity from the surface of a C<sub>22</sub>OH:PD(5%) mixture melt at the different temperatures and for the different surface phases indicated. Inset: the x-ray reflectivity at a constant  $q_z = 0.25 \text{ \AA}^{-1}$  and for varying  $T$ .

diolation. At slightly higher  $T = 69^\circ\text{C}$ , a new and markedly different  $R(q_z)$  is observed. The modulation period is now twice that of the bilayer, indicating a new, *monolayer*, surface-frozen phase. XR, GID, and BR data [9] reveal the structure for the two surface phases described below.

*3.2.1. The monolayer phase.* Model fits to the measured  $R(q_z)$  confirm the layer to be monomolecular [9]. GID shows that it is crystalline, with hexagonal, untilted (except for  $\text{C}_{28}\text{OH}$ ), molecular packing and an intermolecular spacing varying slightly from 4.94 Å for  $n = 20$  to 4.87 Å for  $n = 28$ , as compared to 4.83 Å for the untilted bilayer phase of pure alcohols [3]. The hydroxyl groups of the molecules point into the liquid, forming a hydrophilic, OH-terminated surface, onto which the PD molecules can be expected to segregate. Indeed, the model fits reveal at the monolayer/liquid interface an increased electron density decaying to the bulk  $\rho_e$ -value over a distance of a few Å. This excess density increases with  $\phi$ , as expected of an adsorbed layer. At a given  $\phi$ , the excess density decreases with increasing  $m$ . This supports the adsorption hypothesis, since while the number of diols adsorbing remains the same, the average number of the dense hydroxyl groups per  $\text{CH}_2$  group decreases with increasing  $m$ , thus reducing the density. The adsorbing diols compete with the alcohol molecules for the hydrogen-bonding sites at the bottom of the monolayer. Since a diol has two hydroxyls, and the alcohol just one, and since  $m \ll n$ , the diols have more OH groups per  $\text{CH}_2$ . Thus, above a certain  $\phi$  the diols prevail, covering the monolayer's bottom, preventing the hydrogen bonding of alcohols and the formation of the second alcohol layer. This implies, in turn, that the monolayer phase should occur only above a certain critical concentration  $\phi_{crit}$ , and since the number of hydroxyls per  $\text{CH}_2$  decreases with  $m$ ,  $\phi_{crit}$  should increase with  $m$ . Both effects are indeed observed, as discussed below.

*3.2.2. The bilayer phase.* The  $R(q_z)$  curves in figure 2 show the diolated bilayer's structure to be very similar to that of the pure alcohol. The modelling yields a small increase ( $< 1$  Å) in the bilayer's thickness which, however, is within the experimental uncertainty. For mixtures with  $n < 22$ , where the molecules are untilted, an intermolecular distance of 4.90 Å is observed by means of GID for all  $n$ , slightly larger than the 4.83 Å found for pure alcohols. No variation with  $\phi$  is observed for either the mono- or the bilayer spacings [9]. However, for the tilted phases at  $n \geq 24$  another novel effect is observed: a continuous, monotonic tilt variation as  $\phi$  is varied. For example, for pure  $\text{C}_{28}\text{OH}$  the molecules in the SF bilayer are tilted by  $\sim 20^\circ$  from the surface normal while increasing the PD  $\phi$  to 12% reduces the tilt to  $13^\circ$  [3]. The tilt variation is driven, most probably, by the varying hydrophilicity of the subphase due the OH-rich PD concentration changes. This varies the bilayer-subphase interaction, leaving the in-plane chain-chain interaction and the hydrogen bonding of the two layers unchanged. The variation in the balance between these interactions varies the tilt.

*3.2.3. The phase diagram.* Measuring the variation of  $R(q_z)$  with  $T$  at a judiciously chosen fixed  $q_z$  allows one to determine the surface phase transition temperatures and the transition's order, and also monitors  $T$ -variations, if any, in the SF layer's structure within each surface phase. Such so-called  $T$ -scans are shown in figure 2's inset. The two highest- $T$  jumps mark the liquid/monolayer and monolayer/bilayer transitions, respectively. The lowest- $T$  jump indicates the bulk freezing at  $T_f$ , where the surface roughens macroscopically and the XR drops abruptly to near-zero. The sharpness of all jumps shows them to be first-order transitions. The existence range,  $\Delta T$ , of each phase is observed to vary significantly with  $\phi$ . A small change in  $T_f$  is also observed. The surface phase behaviour depends, thus, on both  $T$  and  $\phi$  and also on the

diol's chain length  $m$ , as discussed above.

Our x-ray and surface tension measurements [9] yield the  $(T, \phi, m)$  phase diagram in figure 3. The monolayer phase appears only above some critical concentration  $\phi_{crit}$ ,  $\sim 5\%$  for 1, 3-propanediol ( $m = 3$ ) and  $\sim 10\%$  for 1, 7-heptadiol ( $m = 7$ ). For 1, 9-nonadiol ( $m = 9$ ) no monolayer phase is observed, presumably since  $\phi_{crit}$  is higher than the  $\phi \sim 20\%$  where macroscopic phase separation of the diol and alcohol occurs for all  $m$ , and prevents meaningful measurements.  $\Delta T_{monolayer}$  decreases with  $m$  for a given  $\phi$ , indicating a reduction in the phase's stability. Still, these  $\Delta T_{monolayer} \sim 5^\circ\text{C}$ , are among the highest observed in any material showing SF. The increase in  $\phi_{crit}$  and decrease in stability are in line with the diol adsorption at the monolayer's bottom, as discussed above. Finally, the phase boundaries are determined by the balance between the various surface energies occurring for each of the phases. Calculations based on this [9] account quantitatively for the observed phase boundaries, and also provides estimates for the values and  $\phi$ -dependence of the layer/melt and layer/vapour surface tensions, quantities not accessible to direct measurements. Further details will be published elsewhere [9].

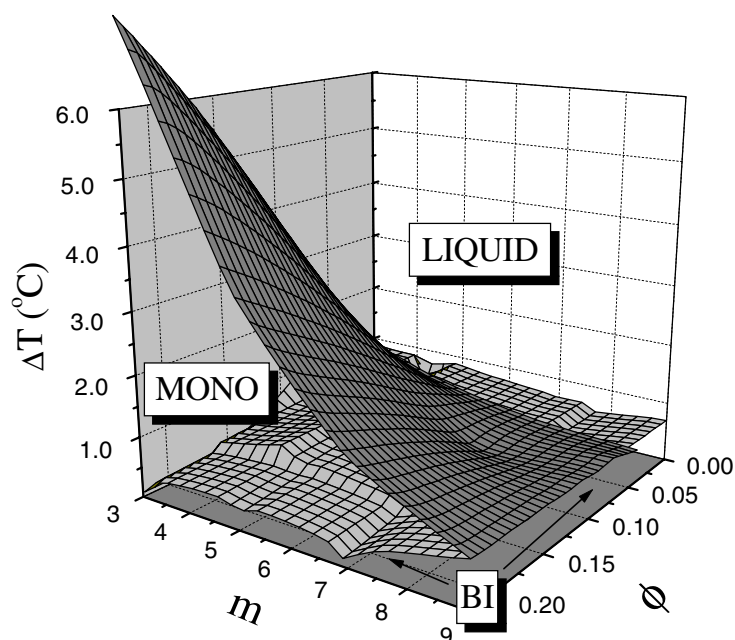


**Figure 3.** The surface phase diagram of diol:C<sub>20</sub>OH melts.  $\Delta T$ , the temperature existence range, is relative to the bulk freezing temperature  $T_f$ ,  $\phi$  is the concentration and  $m$  is the diol's chain length.

#### 4. Conclusions

The role of HB between alcohol and additive molecules in the SF layer was studied. Water intercalates into the SF bilayer's centre with a molecular water:alcohol ratio  $\sim 1:2$ , causing a  $\sim 2.5 \text{ \AA}$  swelling, and increasing the bilayer's stability range in  $n$  and  $\Delta T$ . Diols, due to their hydrophobic alkyl chain, do not penetrate into the bilayer. However, by changing the bilayer/liquid interfacial energy, they change the molecular tilt in the bilayer commensurately

with  $\phi$ . This is exclusively a surface effect for which no parallel bulk behaviour was observed [9]. The appearance of a new monolayer surface phase, having, again, no parallel in the bulk phases, was also observed. Finally, the surface phase diagram of the alcohol:diol melt was determined; it showed an increase in  $\phi_{crit}$  and a decrease in the monolayer phase's stability range with diol length, as expected from the suggested mechanism for the monolayer's formation. The ability to 'engineer' the surface-frozen layer's structure at the molecular level, which was demonstrated here, deserves further study and may have profound implications for both basic science and future practical applications.

### Acknowledgments

Support of the work at Bar-Ilan University by Exxon Research and Engineering Company is gratefully acknowledged, as is the beamtime allocation by NSLS. Brookhaven National Laboratory is supported by the DOE under contract DEAC02-98CH10886.

### References

- [1] Wu X Z *et al* 1993 *Phys. Rev. Lett.* **70** 958  
Wu X Z 1993 *Science* **261** 1018  
Earnshaw J C and Hughes C J 1992 *Phys. Rev. A* **46** R4494
- [2] Ocko B M *et al* 1997 *Phys. Rev. E* **55** 3164
- [3] Deutsch M *et al* 1995 *Europhys. Lett.* **30** 283  
Gang O *et al* 1998 *Phys. Rev. Lett.* **80** 1264  
Gang O 1998 *Phys. Rev. E* **58** 6068
- [4] Kaganer V M *et al* 1999 *Rev. Mod. Phys.* **71** 779
- [5] Ulman A 1991 *An Introduction to Ultrathin Organic Films: from Langmuir-Blodgett to Self Assembly* (Boston, MA: Academic)
- [6] Sirota E B and Wu X Z 1996 *J. Chem. Phys.* **105** 7763
- [7] Deutsch M and Ocko B M 1998 X-ray and neutron reflectivity *Encyclopedia of Applied Physics* vol 23, ed G L Trigg (New York: VCH)  
Russell T P 1990 *Mater. Sci. Rep.* **5** 171
- [8] Ocko B M *et al* 1994 *Phys. Rev. Lett.* **72** 242
- [9] Gang O *et al* 1999 *Phys. Rev. Lett.* **82** 588  
Gang O *et al* 2000 to be published